Electronic Supplementary Information

Thermally Reversible Single-Crystal to Single-Crystal Transformation of Mononuclear to Dinuclear Zn(II) Complexes By[2+2] Cycloaddition Reaction

*Raghavender Medishetty, Terence Teck Sheng Yap, Lip Lin Koh and Jagadese J. Vittal**

Department of Chemistry, National University of Singapore,
3, Science Drive 3, Singapore 117543.
email: *chmjjv@nus.edu.sg*, Fax: (+65)6779-1691

Table of contents

Experimental details:

All the chemicals and solvents were of reagent grade and purchased from different commercial resources and used without further purification. 4spy and 2F-4spy were synthesized according to a reported procedure.[1] Powder X-ray diffraction (PXRD) data were recorded on a D5005 Siemens X-ray diffractometer with graphite monochromatized Cu Kα radiation (λ = 1.54056 Å) at room temperature (298 K). NMR spectra were recorded on a 300 MHz FT-NMR spectrometer with TMS as an internal reference in D_6-DMSO solution. Thermogravimetric analysis (TGA) was performed under nitrogen atmosphere with a heating rate of 5˚C min^{-1} on a TA instruments SDT-2960. Differential scanning calorimetry (DSC) was performed under nitrogen atmosphere with a heating rate of 5˚C min^{-1} on a TA instruments DSC-2920 from room temperature to 300 ˚C. The UV absorption spectral measurements were conducted on a SHIMADZU UV-2450 UV-VIS Spectrophotometers. The photoluminescence spectral measurements were conducted on a HORIBA Jobin Yvon Fluoromax-4 spectrofluorometer by dissolving the compound in DMF at room temperature in air using an excitation wavelength of 300 nm. The C, H, N analysis were carried using Elementar Vario Micro Cube instrument at the Elemental Analysis Lab, CMMAC, Department of Chemistry, National University of Singapore.

All the UV irradiation experiments were conducted in a LUZCHEM UV reactor. In case of crystalline powders, the ground single crystals were packed in between the glass sides placed in the UV reactor. These glass slides were flipped back at regular intervals of time to maintain the uniform exposure of UV radiation.

Preparation of 1: Light yellow single crystals, $[ZnBr_2(4spy)_2]$ have been harvested within two days by careful layering of the methanolic solution of 4-styrylpyridine (4spy, 9.1 mg, 0.05 mmol) over an aqueous solution of $ZnBr_2.2H_2O$ (6.5 mg, 0.025 mmol) using 1-propanol as the buffer and washed with methanol and dried at room temperature. Yield: 5.8 mg (39.7%). ^{1}H-NMR (D_6-DMSO. 300 MHz, 298 K): δ = 8.54 (d, 2H, pyridyl protons of 4spy), 7.2-7.7 (m, 9H, aromatic protons of 4spy), Melting of the compound has not been observed, below its decomposition temperature (250 ˚C). Elemental analysis (%) Calcd for $C_{26}H_{22}N_2Br_2Zn$ (587.67): C, 53.14; H, 3.77; N, 4.77. Found: C, 53.44; H, 3.59; N, 4.73.

Preparation of 2: Dark yellow single crystals of $[Zn_2Br_4(4spy)_2($*rctt*-ppcb$)]$ were obtained by irradiating the single crystals of **1** under UV light for 24h in a Luzchem reactor at 365 nm. ^{1}H-NMR (D_6-DMSO. 300 MHz, 298 K): δ = 8.54 (d, 2H, pyridyl protons of 4spy); 8.30 (d, 2H pyridyl protons of *rctt*-ppcb); 4.60 (s, 2H, cyclobutane protons of *rctt*-ppcb); 6.8- 7.7 (m, aromatic-9H of 4spy, 14H of *rctt*-ppcb). Melting of the compound has not been observed.

Preparation of 2′: Light yellow crystalline [$ZnBr_2$(2F-4spy)(*rctt*-F-ppcb)$_{0.5}$] was obtained instead of **5** by mixing the methanolic solution of 2F-4spy (10.0 mg, 0.05 mmol), *rctt*-F-ppcb (10 mg, 0.025 mmol) and $ZnBr_2.2H_2O$ (13.0 mg, 0.05 mmol) and washed with excess methanol and dried at room temperature. ^{1}H-NMR (*D*$_6$-DMSO. 300 MHz, 298 K): δ = 8.54 (d, 2H, pyridyl proton of 2F-4spy), 8.30 (d, 2H, pyridyl protons of *rctt*-F-ppcb), 4.65 (s, 4H, cyclobutane protons of *rctt*-F-ppcb); 6.8- 7.7 (m, aromatic-8H of 2F-4spy, 12H of *rctt*-F-ppcb). Melting of the compound has not been observed. Elemental analysis (%)Calcd for $C_{26}H_{22}N_2Br_2Zn$ (587.67): C, 53.14; H, 3.77; N, 4.77. Found: C, 53.41; H, 3.64; N, 4.74.

Preparation of 1′: The single crystals of **2** were heated at 220°C for 48 h. ^{1}H NMR (*D*$_6$-DMSO. 300 MHz, 298 K): δ = 8.54 (d, 2H, pyridyl protons of 4spy), 7.2-7.7 (m, 9H aromatic protons of 4spy).

Preparation of 3: The powdered **1** was packed between the slides and irradiated under UV light by flipping the slides at regular intervals of 12 h. ^{1}H-NMR (*D*$_6$-DMSO. 300 MHz, 298 K): δ = 8.30 (d, 2H, pyridyl protons of *rctt*-ppcb), 4.60 (s, 2H, cyclobutane protons of *rctt*-ppcb); 6.8- 7.7 (m, 14H, aromatic protons of *rctt*-ppcb). Melting of the compound has not been observed.

Preparation of 4: Compound [$ZnBr_2$(2F-4spy)$_2$] was synthesized similar to **1,** but 2F-4spy was used instead of 4spy ligand. Light yellow single crystals of **4** were harvested within a few days and washed with methanol and dried at room temperature. Yield: 6.5 mg (42%). ^{1}H-NMR (*D*$_6$-DMSO. 300 MHz, 298 K): δ = 8.54 (d, 2H, pyridyl proton of 2F-4spy), 7.2-7.8 (m, 8H aromatic protons of 2F-4spy). Melting of the compound has not been observed. Elemental analysis (%) Calcd for $C_{26}H_{20}N_2Br_2F_2Zn$ (623.67): C, 50.07; H, 3.23; N, 4.99. Found: C, 50.01; H, 3.05; N, 4.45.

Preparation of 5: Obtained by the UV irradiation of single crystals of **4** for about 18 h. ^{1}H-NMR (*D*$_6$-DMSO. 300 MHz, 298 K): δ = 8.54 (d, 2H, pyridyl proton of 2F-4spy), 8.30 (d, 2H, pyridyl protons of *rctt*-F-ppcb), 4.65 (s, 4H, cyclobutane protons of *rctt*-F-ppcb); 6.8- 7.7 (m, aromatic-8H of 2F-4spy, 12H of *rctt*-F-ppcb). Melting of the compound has not been observed.

Preparation of 5′: Light yellow crystalline [ZnBr$_2$(2F-4spy)(*rctt*-F-ppcb)$_{0.5}$] was obtained instead of **5** by mixing the methanolic solution of 2F-4spy (10.0 mg, 0.05 mmol), *rctt*-F-ppcb (10 mg, 0.025 mmol) and ZnBr$_2$.2H$_2$O (13.0 mg, 0.05 mmol) and washed with excess methanol and dried at room temperature. ^{1}H-NMR (*D*$_6$-DMSO. 300 MHz, 298 K): δ = 8.54 (d, 2H, pyridyl proton of 2F-4spy), 8.30 (d, 2H, pyridyl protons of *rctt*-F-ppcb), 4.65 (s, 4H, cyclobutane protons of *rctt*-F-ppcb); 6.8- 7.7 (m, aromatic-8H of 2F-4spy, 12H of *rctt*-F-ppcb). Melting of the compound has not been observed. Elemental analysis (%) Calcd for $C_{26}H_{20}N_2Br_2F_2Zn$ (623.67): C, 50.07; H, 3.23; N, 4.99. Found: C, 50.20; H, 3.07; N, 4.60.

Preparation of 6: The powdered crystals of **4** were irradiated under UV lamp for 36 h. ^{1}H-NMR (*D*$_6$-DMSO. 300 MHz, 298 K): δ = 8.30 (d, 2H, pyridyl protons of *rctt*-F-ppcb), 4.65 (m, 2H, cyclobutane protons of *rctt*-ppcb); 6.9- 7.4 (m, 12H, aromatic protons of *rctt*-F-ppcb). Melting of the compound has not been observed.

Preparation of 6′: Compound [ZnBr$_2$(*rctt*-F-ppcb)]], was recrystallized from 1:2 (v/v) mixture of DMF/THF. ^{1}H-NMR (*D*$_6$-DMSO. 300 MHz, 298 K): δ = 8.30 (d, 2H, pyridyl protons of *rctt*-F-ppcb), 4.65 (m, 2H, cyclobutane protons of *rctt*-ppcb); 6.9- 7.4 (m, 12H, aromatic protons of *rctt*-F-ppcb). Melting of the compound has not been observed.

Crystallography: Crystal data of all these crystals were collected on a Bruker APEX diffractometer attached with a CCD detector and graphite-monochromated Mo Kα radiation (λ = 0.71073 Å) using a sealed tube at 100(2) K. Absorption corrections were made with the program SADABS,[2] and the crystallographic package SHELXTL[3] was used for all calculations. CCDC 938967-938971 contains the supplementary crystallographic data for this paper. These data can be obtained free of charge from the Cambridge Crystallographic Data Centre via www.ccdc.cam.ac.uk/data_request/cif. The disorders present in **1-6** are described below briefly.

Crystal data of all these crystals were collected on a Bruker APEX diffractometer attached with a CCD detector and graphite-monochromated Mo-Kα radiation (λ = 0.71073 Å) using a sealed tube at 100(2) K. Absorption corrections were made with the program SADABS,[2] and the crystallographic package SHELXTL[3] was used for all calculations. CCDC 938967-938971 contains the supplementary crystallographic data for this paper. These data can be obtained free of charge from the Cambridge Crystallographic Data Centre via www.ccdc.cam.ac.uk/data_request/cif.

[ZnBr$_2$(4spy)$_2$], 1 (CCDC 938967): One of the spy is disordered. The two independent spy ligands (N1 – C13 atoms have been refined to 0.6194(48). The C=C and C-C distances are fixed using DFIX option while soft constraints were applied to other disordered atoms.

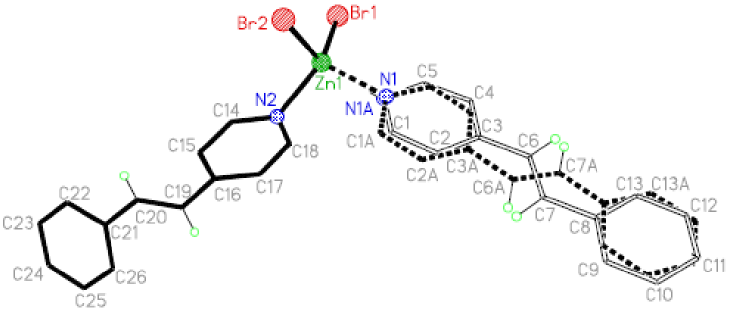

Figure S1. The asymmetric unit of **1** is shown along with the number scheme and disorder in one of the 4spy ligands.

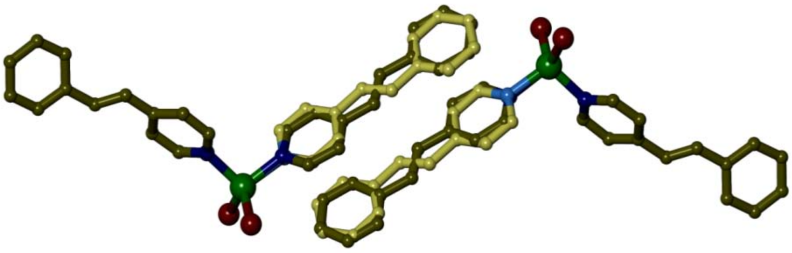

Figure S2. A ball and stick diagram is showing the relative orientations of the disordered 4spy in the solid state structure of **1**.

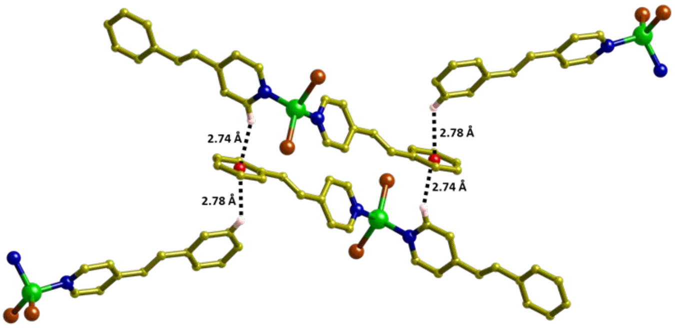

Figure S3. CH···π (aromatic ring) interaction observed in **1.** The centroids are shown as red balls. The H-atoms are not shown for clarity.

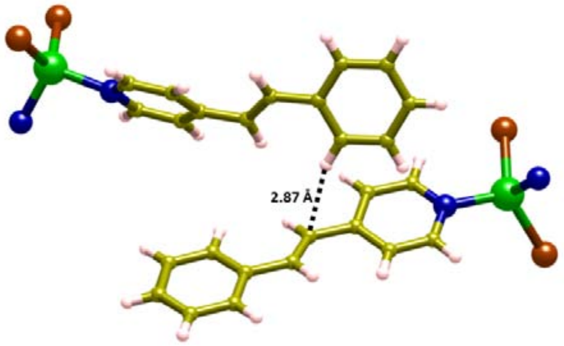

Figure S4. CH···π (olefin) interaction in **1.**

[Zn_2Br_4(*rctt*-ppcb)(4spy)$_2$], 2 (CCDC 938968): The center of cyclobutane is at the crystallographic inversion center. The cyclobutane ligand *rctt*-ppcb (N2, C14-C26) is disordered. Two independent components were refined to 0.594(15). The cyclobutane rings is constrained using DFIX option.

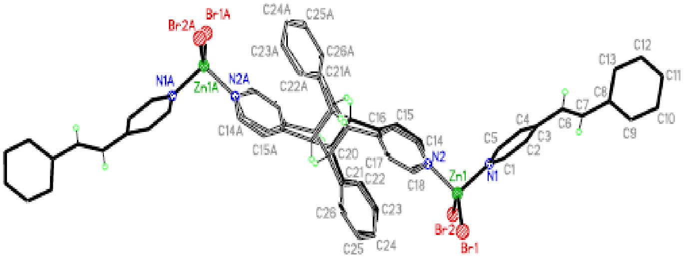

Figure S5. Molecular structure of **2** is shown along with the numbering scheme and disorder in the *rctt*-ppcb ligand. The symmetry operator for the atomic labels with extension 'A': -x, 1-y, -z.

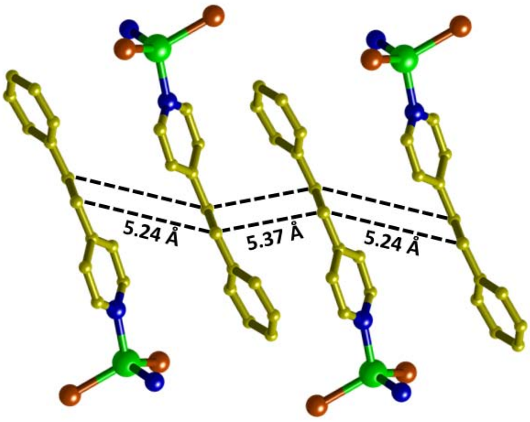

Figure S6. The non-bonded distances between the non-coplanar 4spy ligands are shown. The torsion angle in the 4spy ligands is 58.8°.

[ZnBr$_2$(2F-4spy)$_2$], 4 (CCDC 938969): One of the Fspy ligand was severely disordered. Two disorder components were refined to 0.652(4). Further the F atom is also disordered with H atom. The F atom in the second Fspy ligand is also disordered (0.905(6)). Constraints and restraints were applied to both Fspy ligands in the final model.

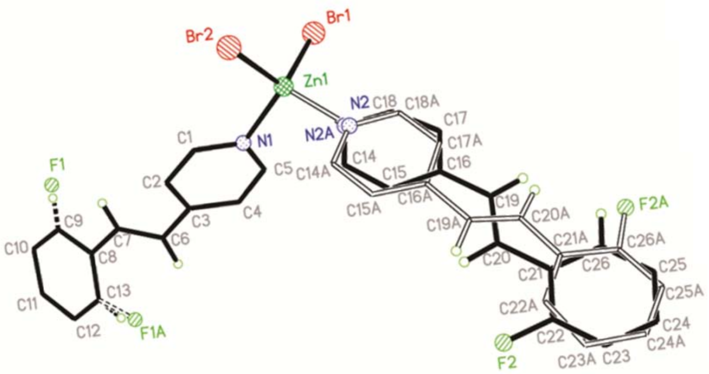

Figure S7. The asymmetric unit of **4** is shown along with the numbering scheme and disorder in the 2F-4spy ligand. The atoms with extension ‘A’ are the minor disordered 2F-4spy ligand.

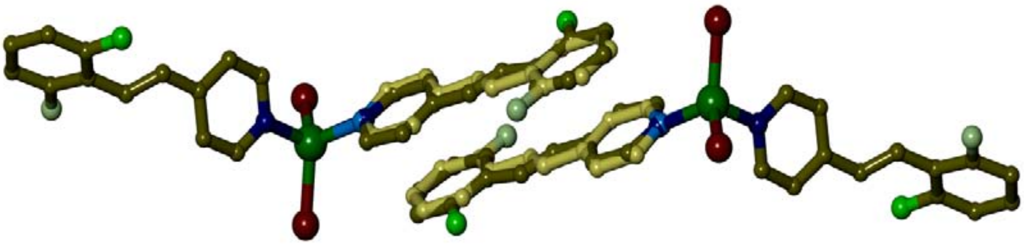

Figure S8. A ball and stick diagram is showing the relative orientations of the disordered 4spy in the solid state structure of **4**.

[Zn$_2$Br$_4$(*rctt*-Fppcb)(2F-spy)$_2$], 5 (CCDC 938970): The *rctt*-Fppcb ligand is disordered. Two different components were included in the structural model and refined to 0.674(6). The cyclobutane bonds were constraints using DFIX option while soft restraints were applied to keep an ideal geometry for these disordered components. In both the ligands, the F and H were found to be disordered. In the 2F-spy ligand, the F disorder component was refined to 0.723(11).

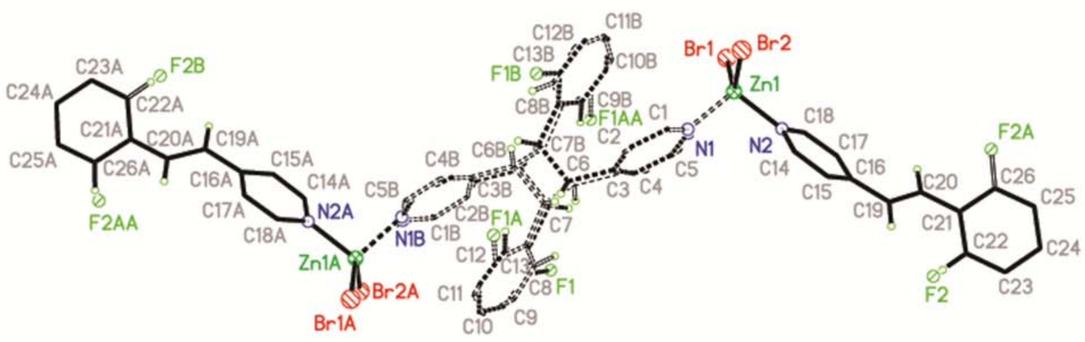

Figure S9. Molecular structure of **5** is showing the numbering scheme and disorder in the *rctt*-F-ppcb ligand. The atoms with extension ‘A’ have symmetry operator -x, 1-y, 1-z (except the disordered F atoms). The atoms with extension ‘B’ are the disordered *rctt* ligand.

Figure S10. A ball and stick diagram is showing the molecular structure of **5** and the disordered *rctt*-Fppcb ligand.

[ZnBr$_2$(*rctt*-Fppcb)$_2$], 6′ (CCDC 938971): Poorly diffracting nature of the polymer is responsible for the poor quality of the data which is in turn responsible for the high agreement factors.

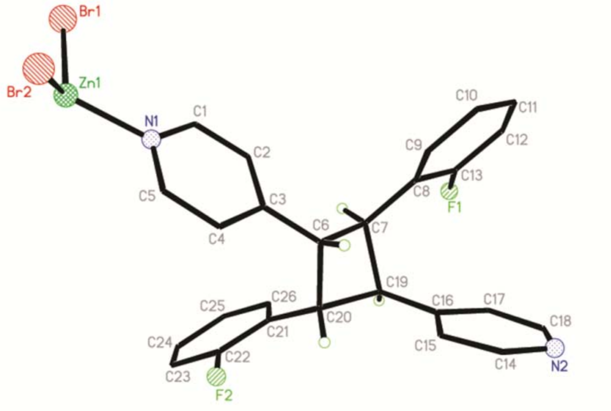

Figure S11. The asymmetric unit of **6′** is shown with the numbering scheme.

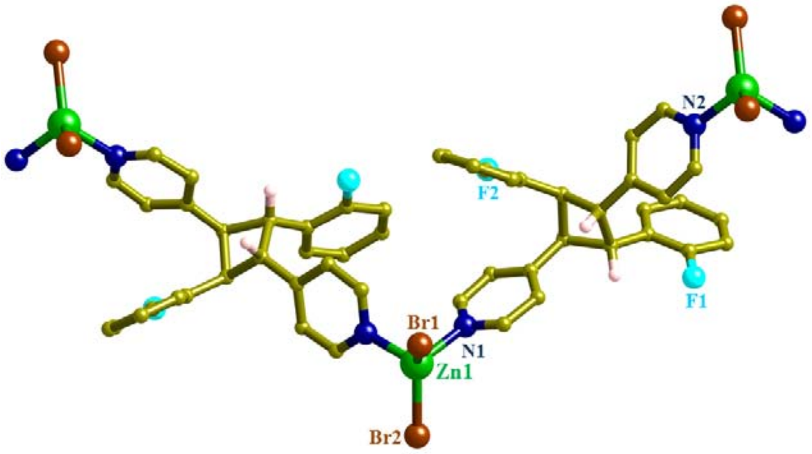

Figure S12. A ball and stick diagram showing the polymer chains of **6**. The H atoms are not shown.

Table S1. Cell data for **1, 2, 4-6’**.

Cell data	**1**	**2**	**4**	**5**	**6′**
Sp. Grp.	$P2_1/n$	$P2_1/n$	$P2_1/n$	$P2_1/n$	$P2_1/n$
a, Å	9.4853(5)	9.5694(12)	9.6230(9)	9.6691(15)	11.015(3)
b, Å	12.9621(6)	13.0123(16)	13.0226(11)	13.252(2)	12.395(4)
c, Å	19.1602(9)	19.216(2)	19.0893(17)	19.137(3)	18.034(6)
β, °	90.917(1)	91.437(3)	90.861(2)	92.175(4)	90.529(8)
V, Å^3	2355.4(2)	2392.0(5)	2391.9(4)	2450.4(7)	2462.2(13)
Z	4	2	4	2	4
d, g.cm^{-3}	1.657	1.632	1.732	1.690	1.682
R_1	0.0293	0.0642	0.0441	0.0632	0.1462
wR_2	0.0703	0.1176	0.1139	0.1478	0.4208

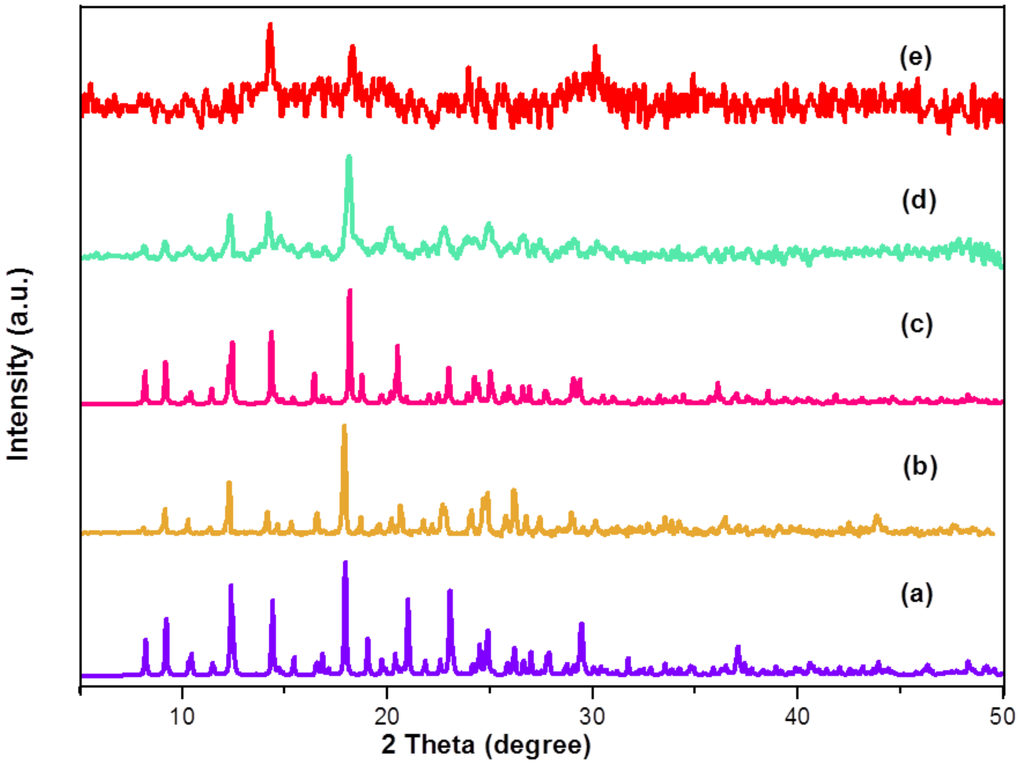

Figure S13. Comparison of PXRD data: (a) simulated from single crystal data of **1**, (b) experimental pattern of **1**, (c) simulated from single crystal data of **2**, (d) experimental pattern of **2**, (e) experimental pattern of **3**.

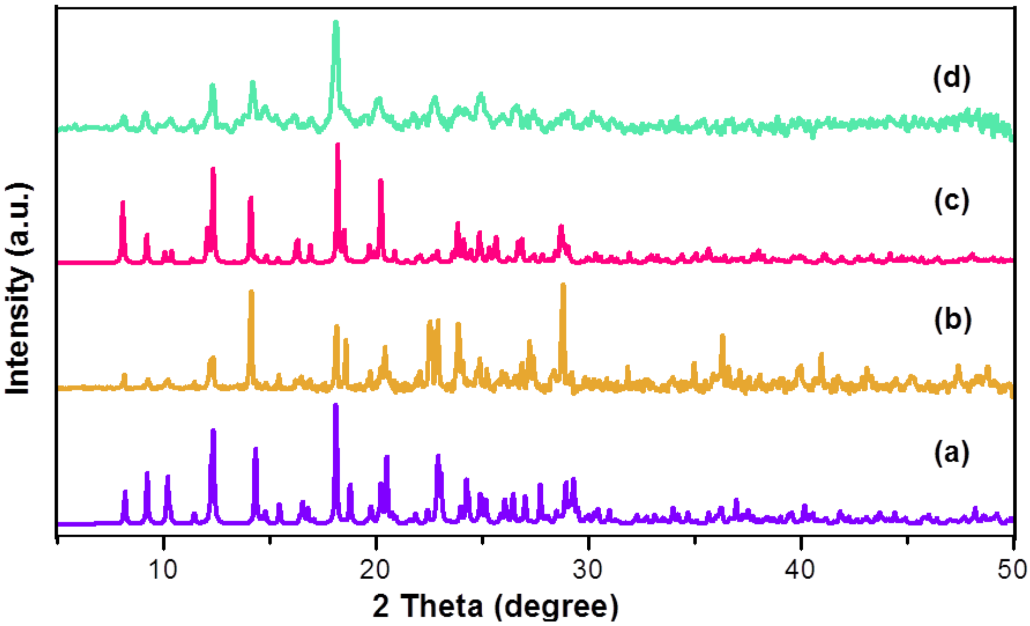

Figure S14. Comparison of PXRD data: (a) simulated from single crystal data of **4**, (b) experimental pattern of **4**, (c) simulated from single crystal data of **5**, (d) experimental pattern of **5**.

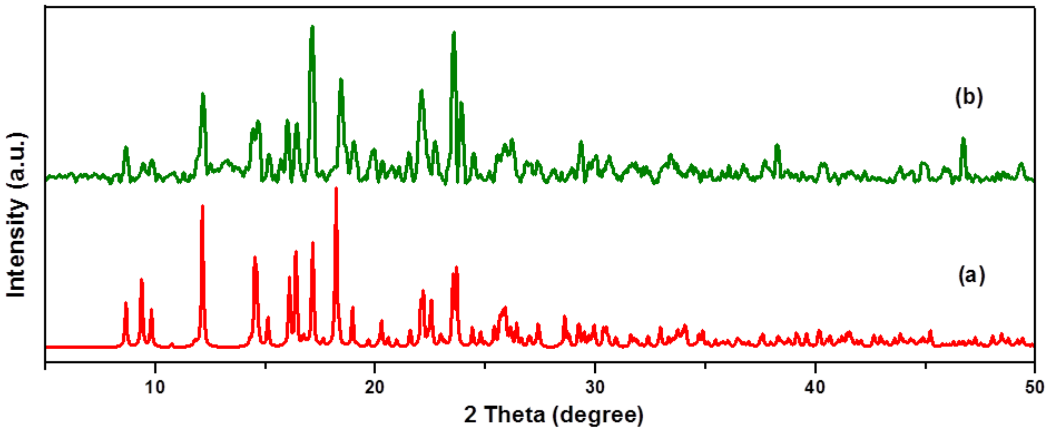

Figure S15. Comparison of PXRD data: (a) simulated pattern from the single crystal data of **6′**, (b) experimentally observed pattern of **6**. The difference in the intensities may be due to preferred orientations of the powder.

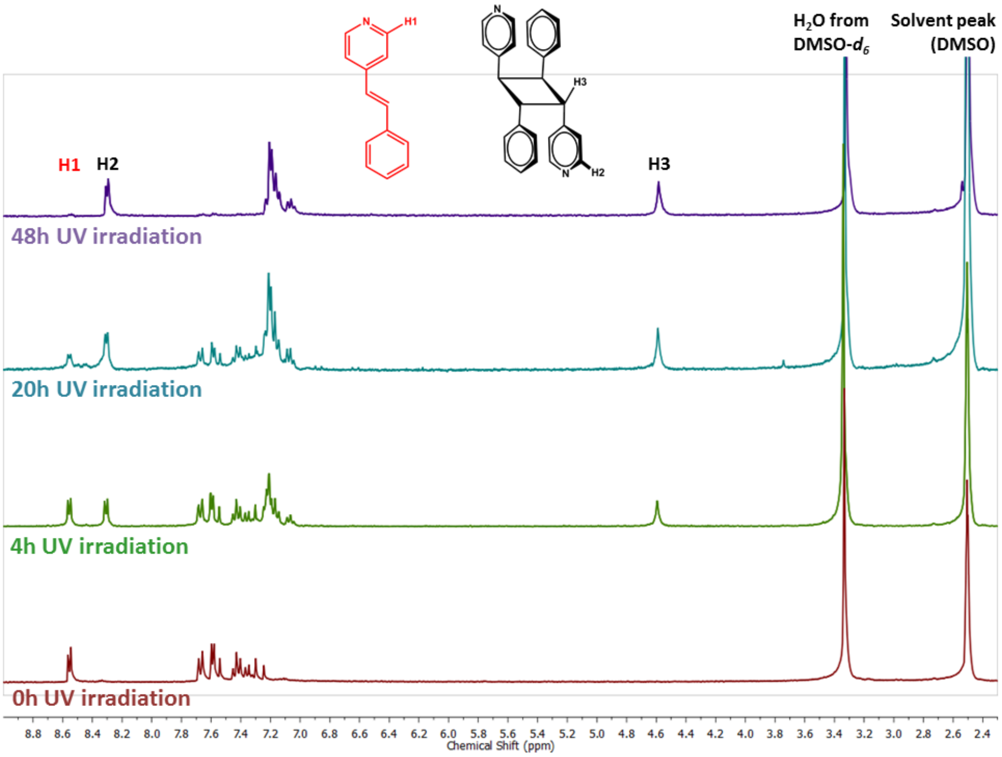

Figure S16. ^{1}H-NMR spectra of **1** in D_6-DMSO**,** subjected to UV irradiation at different intervals of time.

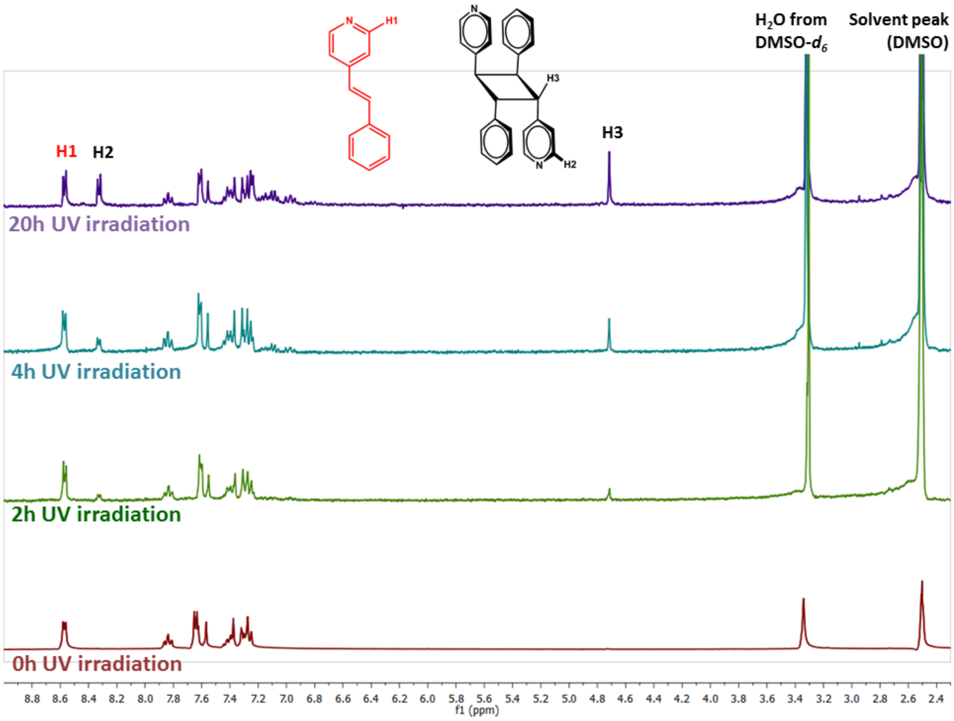

Figure S17. ^{1}H-NMR spectra of <u>single crystals</u> of **1,** in *D*$_6$-DMSO**,** subjected to UV irradiation at different intervals of time.

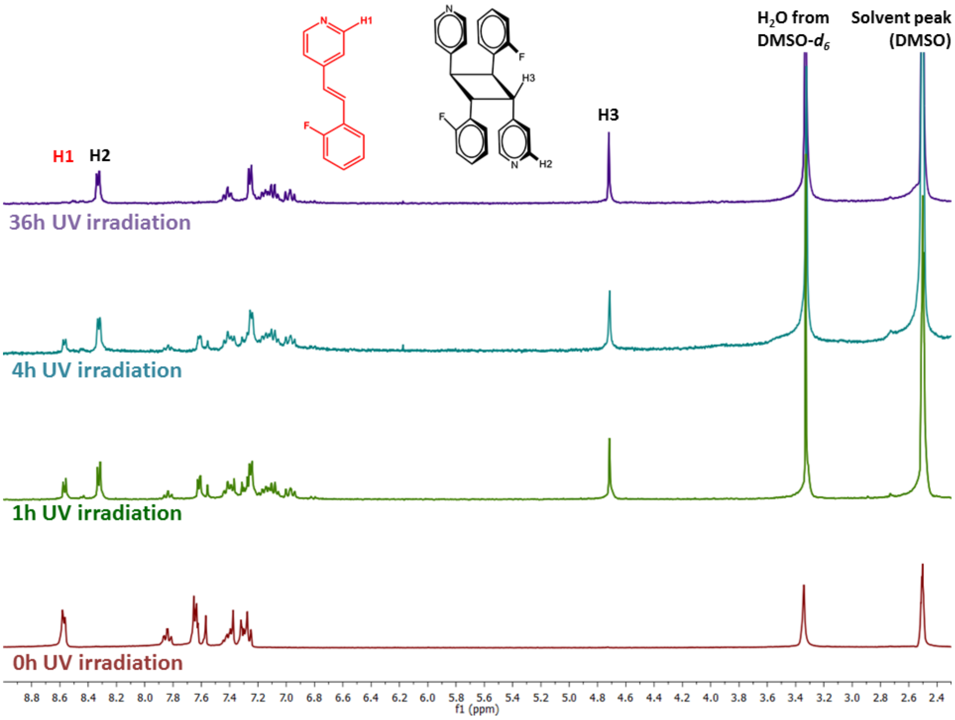

Figure S18. ^{1}H-NMR spectra of **4,** in *D*$_6$-DMSO**,** subjected to UV irradiation at different intervals of time.

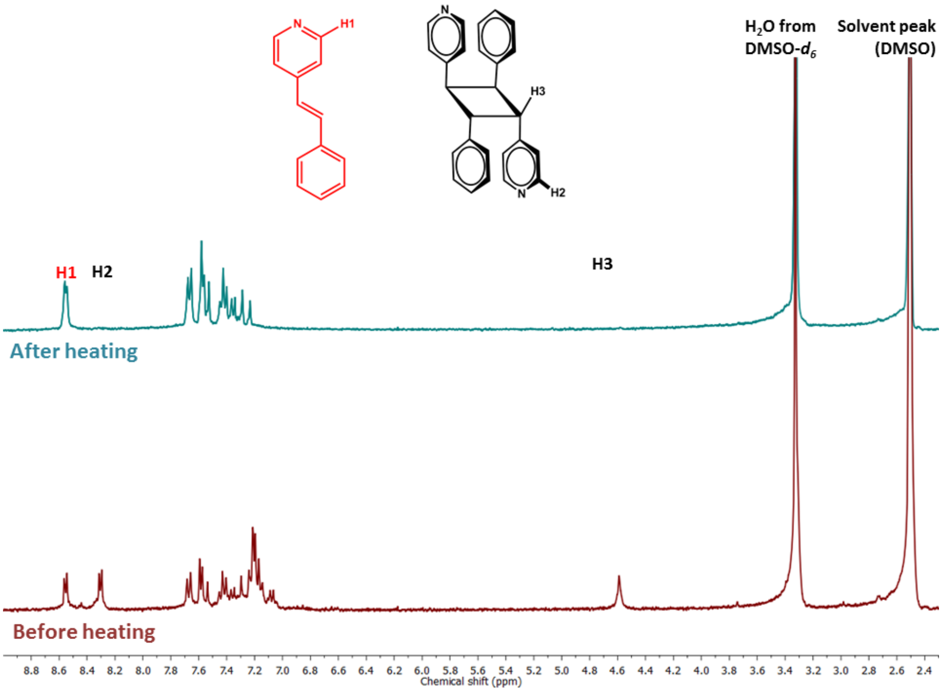

Figure S19. ^{1}H-NMR spectra of **2**, in *D*$_6$-DMSO**,** (a) before and (b) after heating at 220°C for 48 h, showing the formation of **1**.

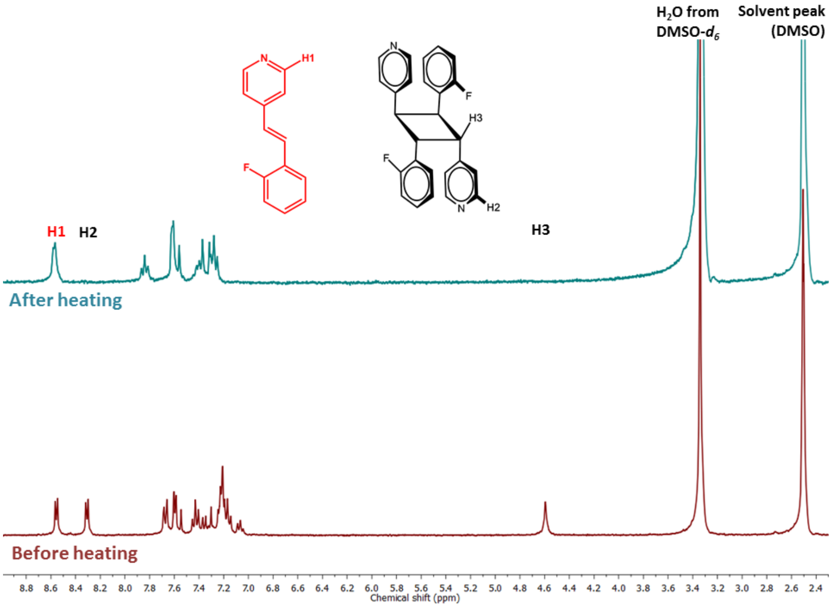

Figure S20. ^{1}H-NMR spectra of **5**, in *D*$_6$-DMSO**,** (a) before and (b) after heating at 220°C for 48 h, showing the formation of **4**.

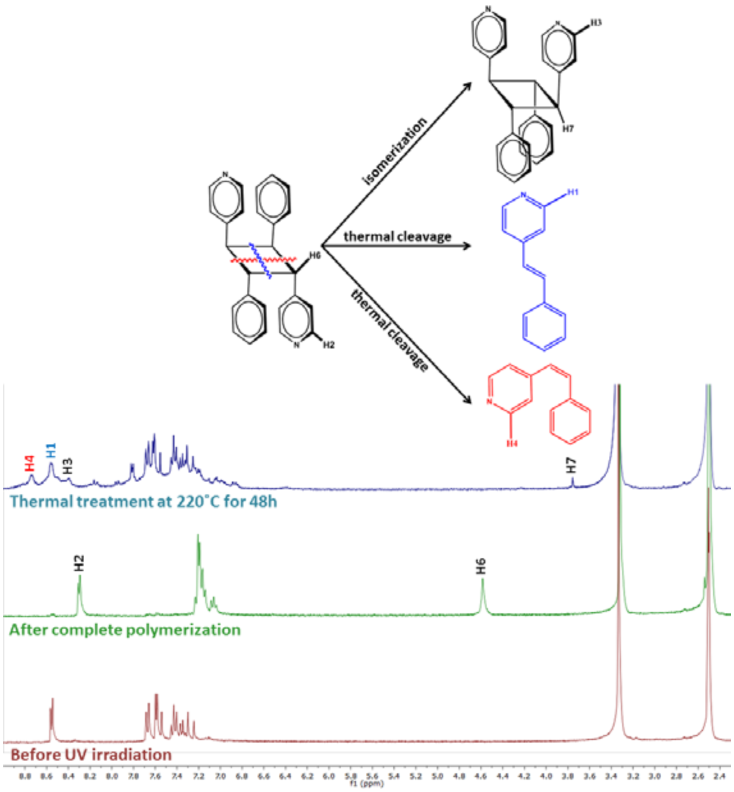

Figure S21. ^{1}H-NMR spectra in D_6-DMSO**,** of (a) metal complex, **1** (b) after complete photo polymerization, **3** and (c) after thermal treatment of the polymer, **3** at 220°C for 48 h showing non stereo specific cleavage of cyclobutane into the both *trans* and *cis* isomers of 4spy (~65 and 25% respectively) along with the isomerization of cyclobutane from *rctt* to *rtct* (~10%).

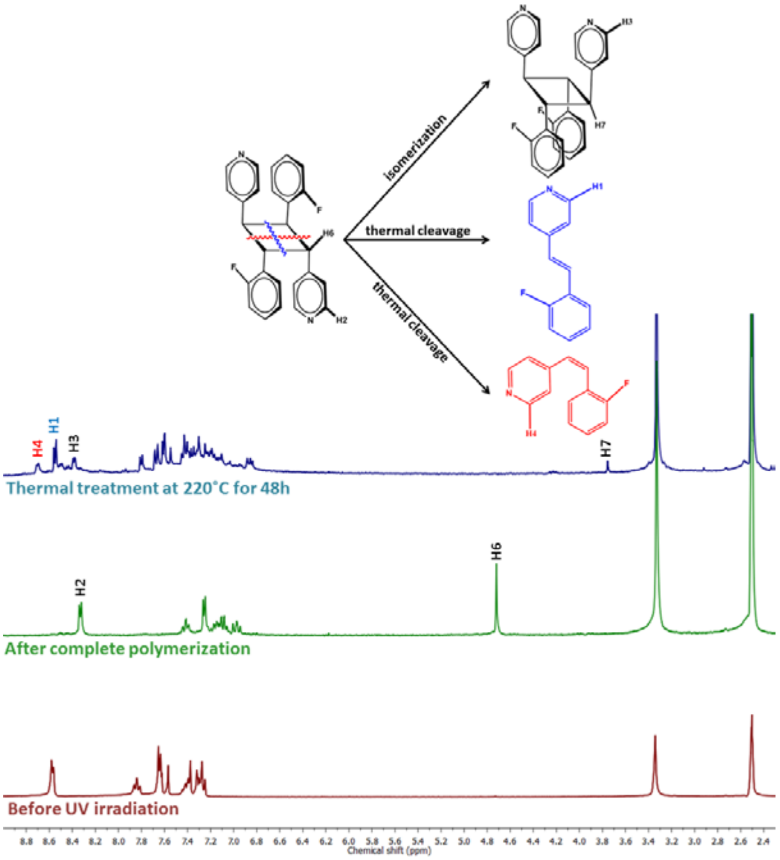

Figure S22. ^{1}H-NMR spectra in D_6-DMSO**,** of (a) metal complex, **4** (b) after complete photo polymerization, **6** and (c) after thermal treatment of the polymer, **6** at 220°C for 48 h showing the non-stereo specific cleavage of cyclobutane similar to **3**.

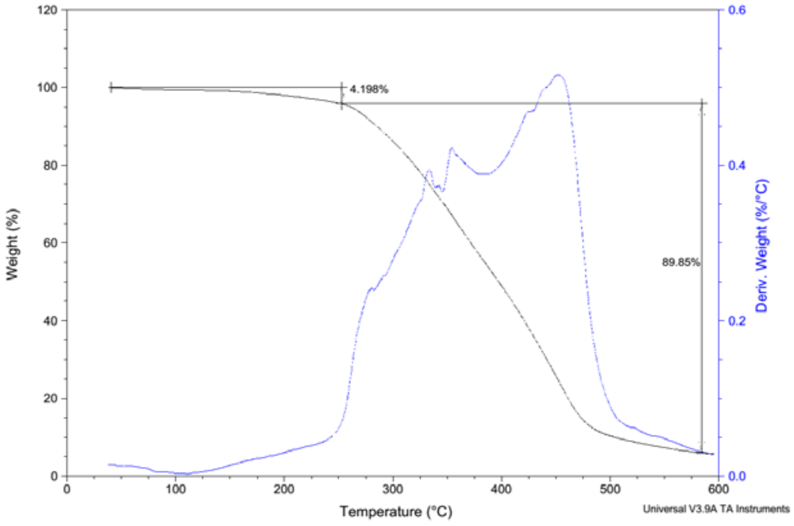

Figure S23. TGA and DTG of compound **1**.

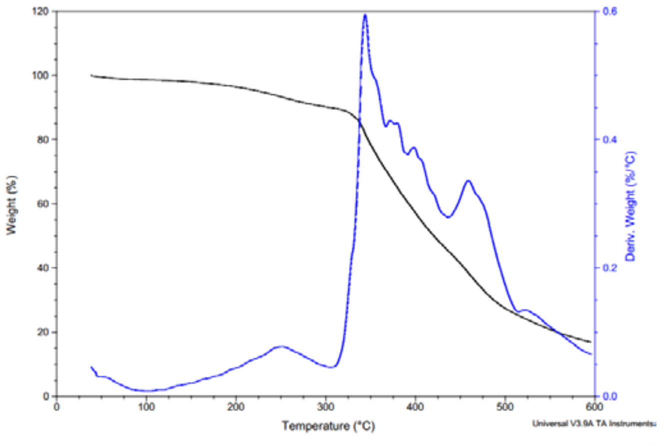

Figure S24. TGA and DTG of compound **3**.

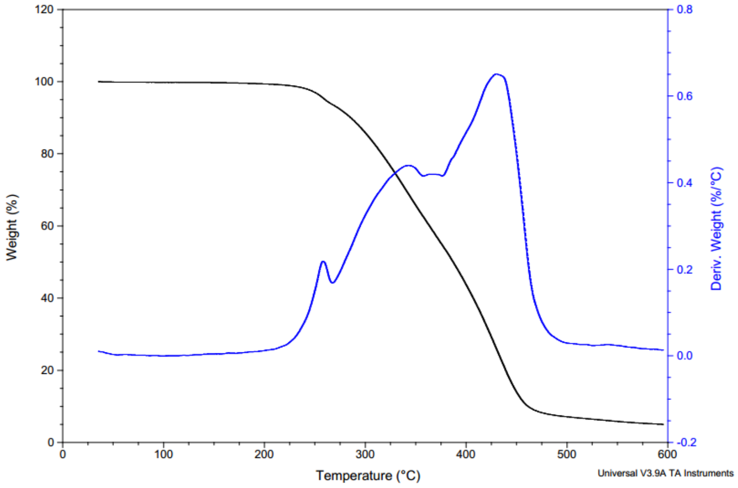

Figure S25. TGA and DTG of compound **4**.

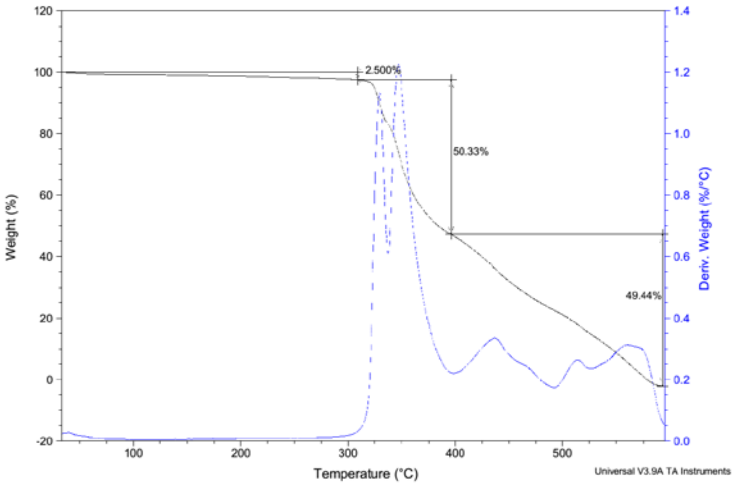

Figure S26. TGA and DTG of compound **6**.

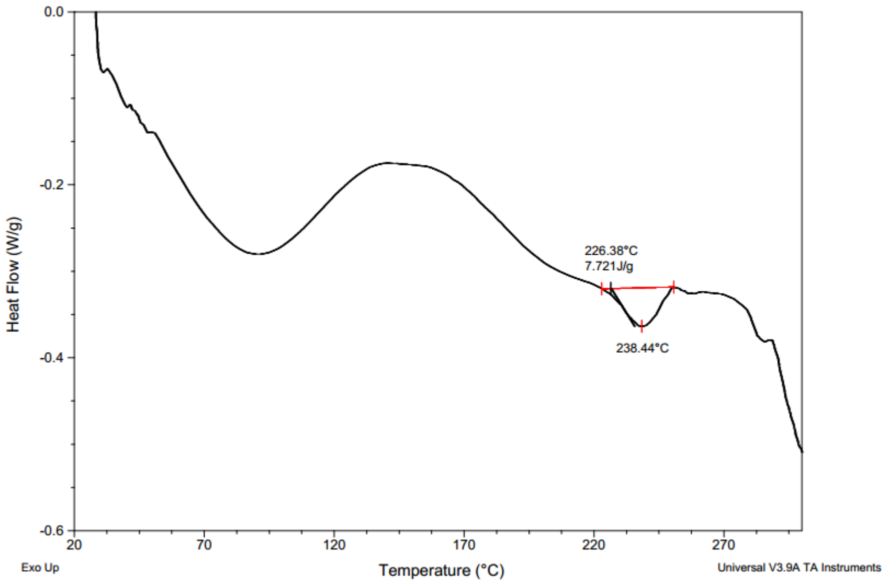

Figure S27. DSC of **2**.

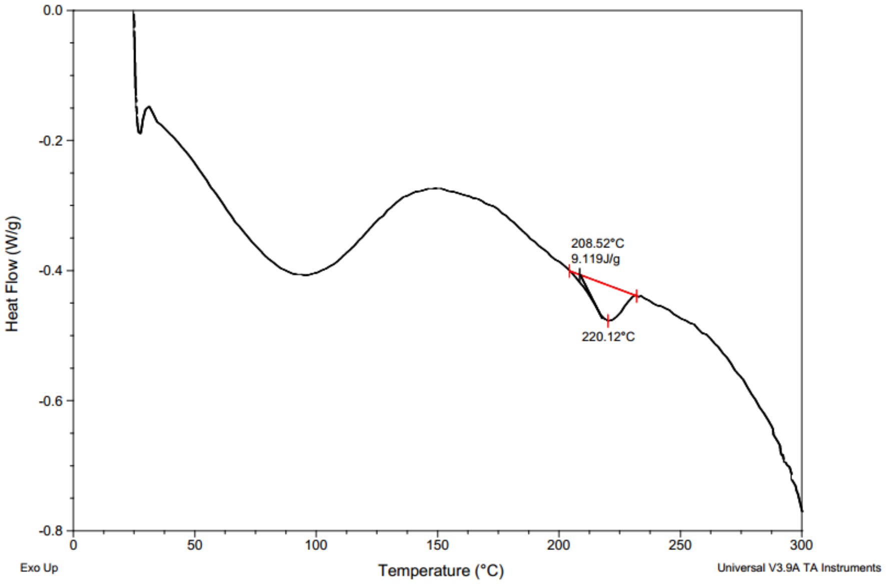

Figure S28. DSC of **5**.

To find the possible transformations at the broad endo and exo thermic peaks below ~200˚C, we heated the single crystals of **2** and **5** at 100˚C and 160˚C for 48 h. But we did not observe any significant deference in ^{1}H NMR. Therefore we concluded that the endothermic after ~200˚C would be responsible for the thermal reversibility.

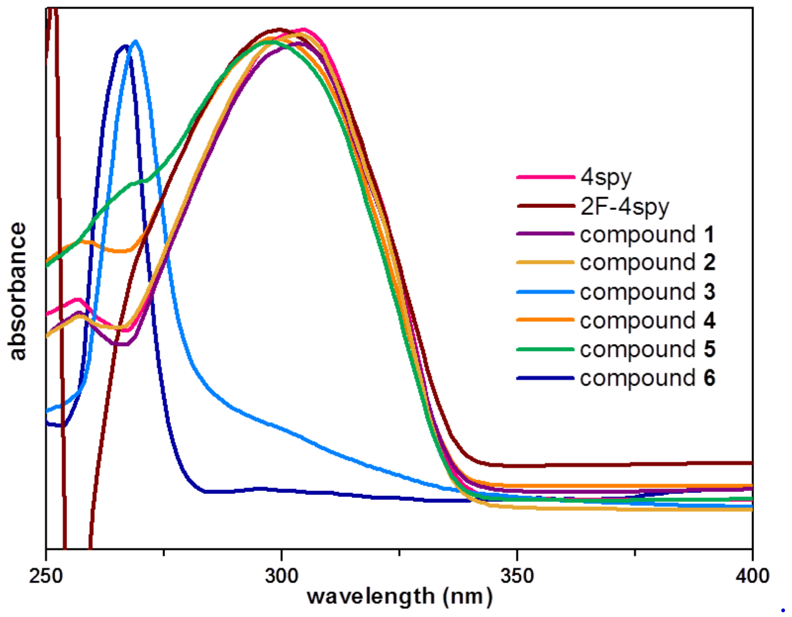

Figure S29. UV-Vis absorption spectra of 4spy and 2F-4spy and **1** to **6** in DMF.

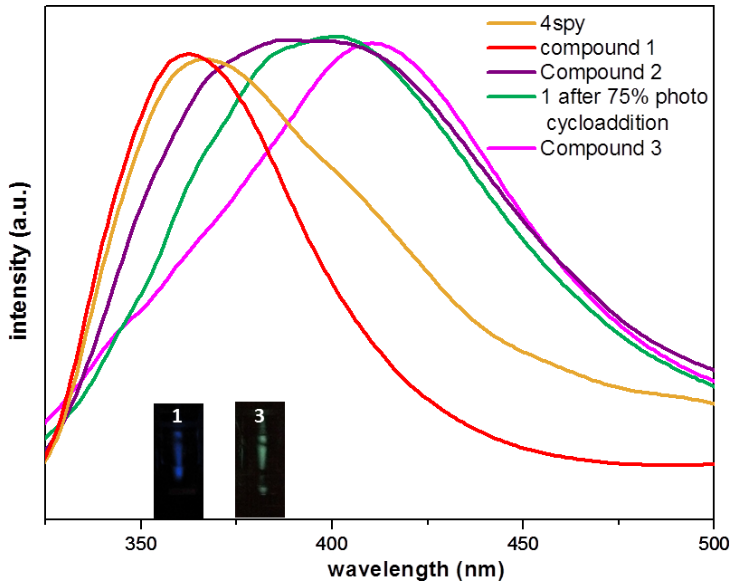

Figure S30. Photoluminescence spectra of compound **1** at different UV irradiation times in DMF (λ_{ex} = 310 nm).

References:

1. (a) L. Horwitz, *J. Org. Chem.*, 1956, **21**, 1039; (b) J. L. R. Williams, R. E. Adel, J. M. Carlson, G. A. Reynolds, D. G. Borden and J. A. Ford, *J. Org. Chem.*, 1963, **28**, 387.
2. G. M. Sheldrick, University of Göttingen, Germany, 1996.
3. (a) G. M. Sheldrick, *Acta Crystallogr. Sect. A.*, 2008, **64**, 112; (b) P. Müller, R. Herbst-Irmer, A. L.Spek, T. R.Schneider and M. R.Sawaya, *Crystal Structure Refinement: A Crystallographer's Guide to SHELXL*, Oxford University Press., 2006.